1987SoPh..114...47K

EMITTING REGION OF SODIUM LINES IN SOLAR PROMINENCES*

KAP-SUNG KIM

Kwasan and Hida Observatories, University of Kyoto, Kyoto, Japan

(Received 16 March, 1987; in revised form 28 September, 1987)

Abstract. We have calculated the emission spectra of hydrogen and sodium atoms in the cool part of prominence models which satisfy simultaneously the constraints of radiative transfer, statistical equilibrium and charge-particle conservations.

In the considered range of our model parameters, emission strengths of Hα and Na I D lines increase with the temperature and the total number density. Low-pressure models raise the ionization rate highly but yield very weak Na I D line intensities, since these model prominences contain small amounts of free electrons and sodium atoms which have a deep relation with the formation of sodium lines. We find that sodium D lines should be emitted in the high pressure region of prominences, and that their intensities are difficult to attain in the cool core of any model prominence with a temperature as low as 4000 K. In order to explain consistently the spectral emissions of Hα and Na I D lines observed in quiescent prominences, a total number density higher than 4×10^{11} cm^{-3} and a temperature over 5000 K are required at least in the cool part of prominences.

1. Introduction

Spectroscopic studies on solar prominences have been carried out theoretically by a number of authors (Hirayama, 1964; Kawaguchi, 1964; Poland *et al.*, 1971; Chultem and Yakovkin, 1974; Heasley and Mihalas, 1976). Among them, Heasley and Mihalas (1976) have achieved a remarkable work on the hydrogen spectrum and the structure of quiescent prominences which satisfy self-consistently the constraints of force and energy balance as well as of radiative transfer and statistical equilibrium of hydrogen atoms. Similar calculations based on the isothermal and isobaric conditions have been made by Heasley and Milkey (1976, 1978, 1983) to construct theoretical models of quiescent prominences with respect to the temperature, density and helium abundance.

In contrast with model structure of prominences simplified as one slab with finite thickness, Fontenla and Rovira (1983) have treated the prominence as a group of numerous slabs characterized by 'filament' or 'thread' confirmed observationally in the earlier works (Dunn, 1960; Engvold, 1978). More recently, Fontenla and Rovira (1985) have presented the result of calculation for the hydrogen lines and continuum emitted by a quiescent prominence with a number of filamentary structures, using the constraints of energy balance and isobaric condition differing little from those of Heasley and Mihalas (1976). Going one step forward from the one dimensional transfer computation of the atmospheric model with an infinite slab geometry. Heasley (1977) has solved the non-LTE line transfer problem in a circularly symmetric, cylindrical region. Two-dimensional transfer calculations of resonance lines in prominence models with an

* Contributions from the Kwasan and Hida Observatories, University of Kyoto, No. 282.

Solar Physics **114** (1987) 47–64.
© 1987 *by Kluwer Academic Publishers.*

© Kluwer Academic Publishers • Provided by the NASA Astrophysics Data System

1987SoPh..114...47K

uniform temperature (T_e = 8000 K) and given ionization degree ($1 < n_p/n_1 < 10$) have been made by Vial (1982b), with the modified code of Mihalas *et al.* (1978).

Interpretation of optically thin line spectra is rather easy without any inclusion of radiative transfer processes, even though we are often confronted with the problem caused by the lack of atomic data. For the optically thin lines of metals (Na, Mg, Sr^+, Ba^+) observed in prominences, statistical equilibrium solutions have been obtained by Landman (1981, 1983, 1984) who used the recent atomic data given by experiments and if not available, his own calculations. In a series of three papers (Landman, 1983, 1984, 1985), he derived the physical conditions in the cool part of prominences such as a low ionization rate of $n(H^+)/n(H\,I) \approx 0.07$, high gas pressure of $P \approx 3$–6 dyn cm^{-2}, temperature of $T \approx 7000$ K and etc. Lately, his results on the ionization degree of hydrogen and the gas pressure were revised to 0.16 and 1.4 dyn cm^{-2}, respectively, by the analysis of the effects of model Na atom level truncation (Landman 1986).

Intensive studies on sodium Na I D lines in solar prominences have been made by Nikaido and Kawaguchi (1983) who performed a non-LTE transfer calculation based on an isothermal slab model with an assumed ionization rate of hydrogen (0.1). They found that the intensity ratio of D1 to D2 emission lines deviates significantly from their theoretical value in some prominences. For this type of prominences, they have shown that the sodium line emitting region should be in high gas pressure and at very low temperature (4000 K), in order to explain the large optical thickness of observed lines.

However, their study should be improved in the following areas. First, the assumed ionization rate of hydrogen atoms may be too high for the cool part of prominences with a temperature as low as 4000 K, even if a thread-like structure of prominences is considered for an easy penetration of Lyman continuum radiation. Second, the distribution of free electrons inside the slab should be taken into consideration, since the number of electrons varies rapidly from the surface hit by EUV radiations to the cool center of prominence. Actually, the distribution of electron density exerts a fair influence on the formation of Na I D lines via the recombination processes. Third, according to observations, comparatively intense emission of Na I D lines is usually accompanied by strong hydrogen Balmer lines. Then, prominence models should be constructed to match successfully such an observational fact.

The purpose of this paper is to investigate the physical conditions of solar prominences which can explain consistently the observed emission spectra of Hα, Hβ, and Na I D lines. In order to take a full account of the above mentioned problem, we have solved the non-LTE problems of hydrogen and sodium atoms simultaneously. We will present the result of our calculation on hydrogen and sodium line emissions for prominence models with isothermal and isobaric slab structure.

2. Method

2.1. Basic equations

The emitting region of sodium lines in solar prominences has been examined by using a stationary model in which ionization and thermal equilibrium is supposed to be

© Kluwer Academic Publishers • Provided by the NASA Astrophysics Data System

1987SoPh..114...47K

satisfied. We consider for simplicity that the prominence embedded into the corona is made up of a cool core with uniform density and temperature inside. The geometry of the cool core we consider is an infinite slab with a finite thickness, symmetrical with respect to the central plane and illuminated on both sides by the incident radiation coming from the photosphere, the chromosphere, the transition region and the corona. We will treat the cool core as a target model of prominence to investigate from now in our work.

The basic equations used in our model are as follows:

Transfer equation:

$$\partial^2(f_\nu J_\nu)/\partial\tau_\nu^2 = J_\nu - S_\nu . \tag{1}$$

Rate equation:

$$\mathrm{d}n_i(X)/\mathrm{d}t = F_i(J_\nu, n_j) - D_i(J_\nu, n_i) . \tag{2}$$

Charge conservation:

$$n_e = \Sigma\, n(X^+) . \tag{3}$$

Particle conservation:

$$N = n_e + \Sigma N(X) . \tag{4}$$

Here f_ν, J_ν, and S_ν are the Eddington factor, mean intensity and source function at frequency ν, respectively. F_i and D_i are the total formation and destruction rates of atomic species X in the excited state of energy level i, which are generally expressed by both radiative and collisional transition processes. $n_i(X)$ is an occupation number for level $i(i \neq j)$. The net rate of n_i, $\mathrm{d}n_i/\mathrm{d}t$ is, of course, set to zero, by the assumption of stationary state. And n_e, $n(X^+)$, $N(X)$, and N stand for the electron number, ion number, number of species X and total particle number density of the model, respectively. In the equation of charge conservation, we ignore the number of free electrons which come from the second ionization stage of the species.

After the transfer equation is transformed to difference equations, all equations are linearized for the perturbations of unknown quantities. And then, we solve simultaneously the full set of above equations, in a similar way described by Auer and Mihalas (1969) and Mihalas (1978).

2.2. Atomic Models

In the present study, we have assumed that the entire prominence material consists solely of hydrogen, sodium atoms and their ions. Hydrogen atoms are the dominant contributor of free electrons in prominences, and our main concern is to see in what physical conditions the observed emission lines of two atomic species with a large difference in ionization potentials and atomic abundances can be explained consistently. Therefore, we may be justified in neglecting the existence of other metallic species.

The hydrogen atomic model used in our work is the four bound levels plus continuum representation. For sodium, we assume 7 levels ($3S_{1/2}$, $3P_{1/2}$, $3P_{3/2}$, $4S_{1/2}$, $3D$, $4P$, $5S_{1/2}$) and continuum. Transition probabilities of both H and Na are taken from Wiese

© Kluwer Academic Publishers • Provided by the NASA Astrophysics Data System

1987SoPh..114...47K

et al. (1966), and collisional rate formulae from Sampson and Golden (1970) and other necessary data from Mihalas (1967) for hydrogen atom. For the radiative and collisional transition rate calculations of sodium, we adopt the same atomic data as listed in Landman (1981, 1983). The sodium abundance relative to hydrogen is taken from the solar elemental abundances of Lambert and Luck (1978).

For incident radiations of Lα and Lβ, we have used the OSO 8 chromospheric line profiles adopted by Vial (1982b) and the total intensity of Lγ observed by Vernazza and Reeves (1978). The continuum radiation fields have been taken from the tabulation given by Heasley *et al.* (1974), and the incident radiations for sodium lines from the observational data given by Pierce and Slaughter (1982). The incident radiation fields are assumed to be isotropic and their means are calculated by using a dilution factor, ignoring the angular dependence of the radiation.

Of the numerous allowed transitions, we treat Lα, Lβ, Lγ, Hα, D1, D2 lines and Lyc as optically thick lines and continuum. All the remaining subordinate continua and line transitions are assumed to be optically thin. For the optically thin transitions, we regard that corresponding incident radiations on the slab surface can penetrate into the prominence without any attenuation. Consequently the contributions of those radiations to the radiative rate are evaluated as fixed values, with no consideration of transfer process. For optically thick lines, we have solved simultaneously the equations of radiative transfer, statistical equilibrium and charge-particle conservations to determine the distribution of mean radiation field, excitation and ionization equilibria of H and Na atoms within the slab of prominence models.

It is desirable that Lyman lines should be calculated precisely, including the partial redistribution and Voigt line profiles. Frequency redistribution effects for Lα line in prominences were pointed out by Milkey *et al.* (1979) to show that intensity profiles of Lα predicted by complete redistribution and partial redistribution computation differ greatly in the wings of the line (see Figure 1 of the paper). But in our calculation, we have assumed for simplicity that the lines are formed by a process of complete redistribution over a Gaussian line profile which is characterized by thermal and microturbulent ($\xi = 5$ km s^{-1}) Doppler broadening.

3. Results

We have constructed a number of isothermal and isobaric models represented by total number density, temperature and thickness as parameters. In our work, 5000 km is assumed as a standard thickness of prominence models. The physical properties of the models we obtained, are summarized in Table I. N, T, and P denote the total particle number per unit volume, temperature and gas pressure of models, respectively. The notation $\langle N(i) \rangle$ and $(N_P/N_H)_{s,c}$ represent the line-of-sight average of occupation numbers in energy state i, and the ratios of proton to neutral hydrogen number N_H at the surface and the center. For dense and cool models with a large variation in the ionization degree from the surface to the center, the average, $\langle N(i) \rangle$ is the value in the inner part of the slab, since the change in populations is generally considerable around

© Kluwer Academic Publishers • Provided by the NASA Astrophysics Data System

1987SoPh..114...47K

TABLE I

Physical properties of model prominences

N	T	P	$\langle N(1)\rangle$	$\langle N(2)\rangle$	$\langle N(3)\rangle$	$\langle N(3S_{1/2})\rangle$	$\langle N(3P_{1/2})\rangle$	$\langle N(3P_{3/2})\rangle$	$\langle N(Na^+)\rangle$	$\langle N_e\rangle$	$(N_p/N_H)_s$	$(N_p/N_H)_c$
3E+10	4000	0.02	1.56E+10	2.06E+02	9.41E+00	1.38E−01	2.67E−04	4.30E−04	6.27E+04	7.19E+09	8.60E−01	2.19E−01
1E+11	4000	0.06	8.48E+10	4.71E+02	2.16E+01	4.84E−01	9.36E−04	1.51E−03	2.09E+05	7.58E+09	6.95E−01	8.03E−03
3E+11	4000	0.17	2.94E+11	3.06E+02	1.40E+01	5.65E−01	1.09E−03	1.76E−03	6.27E+05	2.95E+09	4.90E−01	5.62E−05
1E+12	4000	0.55	9.96E+11	6.30E+02	2.90E+01	1.24E+00	2.40E−03	3.87E−03	2.09E+06	1.94E+09	3.02E−01	1.94E−05
3E+12	4000	1.66	3.00E+12	8.14E+02	3.76E+01	1.93E+00	3.73E−03	6.02E−03	6.27E+06	1.08E+09	1.79E−01	1.94E−05
3E+10	5000	0.02	5.75E+09	4.75E+02	2.21E+01	1.73E−01	3.66E−04	5.92E−04	6.27E+04	1.21E+10	8.81E−01	3.09E−01
1E+11	5000	0.07	8.18E+10	5.15E+02	2.39E+01	4.33E−01	9.17E−04	1.48E−03	2.09E+05	9.11E+09	7.29E−01	1.69E−02
3E+11	5000	0.21	2.88E+11	5.08E+02	2.36E+01	8.55E−01	1.81E−03	2.92E−03	6.27E+05	5.99E+09	5.27E−01	7.80E−03
1E+12	5000	0.69	9.85E+11	7.33E+02	3.42E+01	3.49E+00	7.40E−03	1.20E−02	2.09E+06	7.35E+09	3.30E−01	5.62E−03
3E+12	5000	2.07	2.97E+12	1.27E+03	5.97E+01	1.75E+01	3.71E−02	5.99E−02	6.27E+06	1.23E+10	1.97E−01	3.78E−03
3E+10	6000	0.02	4.82E+09	4.53E+02	2.12E+01	1.43E−01	3.25E−04	5.26E−04	6.27E+04	1.26E+10	8.98E−01	4.67E−01
1E+11	6000	0.08	6.39E+10	1.00E+03	4.74E+01	6.81E−01	1.55E−03	2.51E−03	2.09E+05	1.80E+10	7.46E−01	1.64E−01
3E+11	6000	0.25	2.40E+11	2.66E+03	1.28E+02	3.41E+00	7.76E−03	1.26E−02	6.27E+05	3.01E+10	5.48E−01	1.04E−01
1E+12	6000	0.83	8.85E+11	9.43E+03	4.67E+02	2.17E+01	4.95E−02	8.01E−02	2.09E+06	5.75E+10	3.49E−01	5.98E−02
3E+12	6000	2.49	2.79E+12	2.98E+04	1.50E+03	1.17E+02	2.66E−01	4.31E−01	6.27E+06	1.03E+11	2.14E−01	3.54E−02
3E+10	7000	0.03	3.71E+09	4.46E+02	2.10E+01	1.23E−01	2.98E−04	4.84E−04	6.27E+04	1.32E+10	9.09E−01	7.08E−01
1E+11	7000	0.10	2.34E+10	3.68E+03	1.80E+02	1.20E+00	2.90E−03	4.69E−03	2.09E+05	3.83E+10	7.71E−01	6.28E−01
3E+11	7000	0.29	1.18E+11	2.06E+04	1.04E+03	8.51E+00	2.06E−02	3.35E−02	6.27E+05	9.11E+10	5.78E−01	4.37E−01
1E+12	7000	0.97	5.87E+11	1.05E+05	5.37E+03	6.41E+01	1.56E−01	2.53E−01	2.09E+06	2.07E+11	3.75E−01	2.61E−01
3E+12	7000	2.90	2.20E+12	3.98E+05	2.03E+04	3.71E+02	9.03E−01	1.47E+00	6.27E+06	4.02E+11	2.33E−01	1.55E−01
3E+10	8000	0.03	2.34E+09	4.58E+02	2.18E+01	1.10E−01	2.81E−04	4.56E−04	6.27E+04	1.38E+10	9.20E−01	8.54E−01
1E+11	8000	0.11	6.56E+09	5.01E+03	2.47E+02	1.22E+00	3.12E−03	5.07E−03	2.09E+05	4.67E+10	8.08E−01	9.02E−01
3E+11	8000	0.33	2.95E+10	4.10E+04	2.09E+03	1.06E+01	2.72E−02	4.42E−02	6.27E+05	1.35E+11	6.41E−01	8.31E−01
1E+12	8000	1.10	2.23E+11	3.34E+05	1.71E+04	9.93E+01	2.56E−01	4.17E−01	2.09E+06	3.89E+11	4.39E−01	6.38E−01
3E+12	8000	3.31	1.18E+12	1.79E+06	9.20E+04	6.61E+02	1.73E+00	2.83E+00	6.27E+06	9.08E+11	2.88E−01	4.36E−01

© Kluwer Academic Publishers • Provided by the NASA Astrophysics Data System

1987SoPh..114...47K

TABLE II

Optical properties of model prominences

N	T	τ(Hα)	τ(Hβ)	τ(D1)	τ(D2)	E(Hα)	E(Hβ)	E(D1)	E(D2)	D1/D2
3E+10	4000	6.29E−02	8.85E−03	2.43E−05	4.62E−05	4.841E+04	8.396E+02	2.273E+00	3.661E+00	0.621
1E+11	4000	1.43E−01	2.02E−02	7.93E−05	1.56E−04	1.070E+05	1.912E+03	7.904E+00	1.279E+01	0.618
3E+11	4000	9.33E−02	1.31E−02	9.06E−05	1.80E−04	7.100E+04	1.245E+03	9.193E+00	1.489E+01	0.617
1E+12	4000	1.92E−01	2.70E−02	1.97E−04	3.94E−04	1.403E+05	2.554E+03	2.014E+01	3.264E+01	0.617
3E+12	4000	2.48E−01	3.49E−02	3.06E−04	6.13E−04	1.772E+05	3.293E+03	3.136E+01	5.082E+01	0.617
3E+10	5000	1.34E−01	1.89E−02	2.91E−05	5.41E−05	1.096E+05	2.224E+03	3.137E+00	5.049E+00	0.621
1E+11	5000	1.45E−01	2.05E−02	6.57E−05	1.29E−04	1.181E+05	2.409E+03	7.754E+00	1.255E+01	0.618
3E+11	5000	1.43E−01	2.02E−02	1.26E−04	2.50E−04	1.166E+05	2.377E+03	1.524E+01	2.472E+01	0.617
1E+12	5000	2.07E−01	2.91E−02	5.08E−04	1.01E−03	1.639E+05	3.422E+03	6.218E+01	1.009E+02	0.616
3E+12	5000	3.59E−01	5.05E−02	2.54E−03	5.08E−03	2.668E+05	5.896E+03	3.112E+02	5.045E+02	0.617
3E+10	6000	1.20E−01	1.69E−02	2.33E−05	4.25E−05	1.061E+05	2.392E+03	2.799E+00	4.503E+00	0.622
1E+11	6000	2.65E−01	3.74E−02	9.72E−05	1.89E−04	2.212E+05	5.268E+03	1.314E+01	2.129E+01	0.617
3E+11	6000	7.04E−01	9.91E−02	4.66E−04	9.23E−04	4.891E+05	1.368E+04	6.537E+01	1.062E+02	0.616
1E+12	6000	2.49E+00	3.51E−01	2.93E−03	5.84E−03	9.310E+05	4.355E+04	4.155E+02	6.745E+02	0.616
3E+12	6000	7.87E+00	1.11E+00	1.57E−02	3.13E−02	1.114E+06	9.997E+04	2.220E+03	3.582E+03	0.620
3E+10	7000	1.11E−01	1.57E−02	1.98E−05	3.53E−05	1.056E+05	2.606E+03	2.583E+00	4.152E+00	0.622
1E+11	7000	9.20E−01	1.30E−01	1.62E−04	3.12E−04	6.264E+05	2.070E+04	2.455E+01	3.983E+01	0.616
3E+11	7000	5.13E+00	7.22E−01	1.10E−03	2.16E−03	1.148E+06	8.937E+04	1.738E+02	2.827E+02	0.615
1E+12	7000	2.63E+01	3.70E+00	8.09E−03	1.61E−02	1.495E+06	1.790E+05	1.304E+03	2.116E+03	0.616
3E+12	7000	9.91E+01	1.40E+01	4.65E−02	9.30E−02	1.834E+06	2.017E+05	7.419E+03	1.184E+04	0.627
3E+10	8000	1.09E−01	1.53E−02	1.76E−05	3.06E−05	1.094E+05	2.922E+03	2.443E+00	3.925E+00	0.622
1E+11	8000	1.19E+00	1.67E−01	1.60E−04	3.04E−04	7.743E+05	3.024E+04	2.653E+01	4.308E+01	0.616
3E+11	8000	9.70E+00	1.37E+00	1.30E−03	2.56E−03	1.299E+06	1.503E+05	2.292E+02	3.735E+02	0.614
1E+12	8000	7.90E+01	1.11E+01	1.18E−02	2.36E−02	1.756E+06	2.306E+05	2.139E+03	3.479E+03	0.615
3E+12	8000	4.24E+02	5.98E+01	7.83E−02	1.56E−01	2.053E+06	2.327E+05	1.397E+04	2.210E+04	0.632

© Kluwer Academic Publishers • Provided by the NASA Astrophysics Data System

1987SoPh..114...47K

the surface but negligible in the interior. Table II shows the optical properties of corresponding models concerning the total optical depth, total intensity of line and intensity ratio of D1 to D2. Total emergent intensities of each line are calculated by the formal solution of transfer equation:

$$E = \int_{-\infty}^{\infty} \mathrm{d}\nu \int_{0}^{\tau_\nu} S_\nu(t_\nu) \exp(-t_\nu/\mu)\, \mathrm{d}t_\nu/\mu\,, \tag{5}$$

where radiations emerging normally from the slab are considered only, by putting the projection angle μ to 1.

We find, as shown in Table II, that emissions of all considered lines become stronger, in proportion to the rise of the temperature and density. Compared to the hydrogen lines, the optical depth of D2 line is always below 1, even in the models with high density. Tables also show that the ionization degree of hydrogen at a temperature of 4000 K is quite low, resulting in much weaker intensities of Na I D lines at this temperature than the smallest observed values of Landman (1981) or Nikaido and Kawaguchi (1983). Low pressure models investigated intensively by Heasley and Milkey (1978) yield generally low Na I D line intensities, in spite of the high ionization rate.

We have examined in detail the dense and cool core with total density of $1 \times 10^{12}\ \mathrm{cm}^{-3}$, a temperature of 5000 K and a thickness of 5000 km. Depth depen-

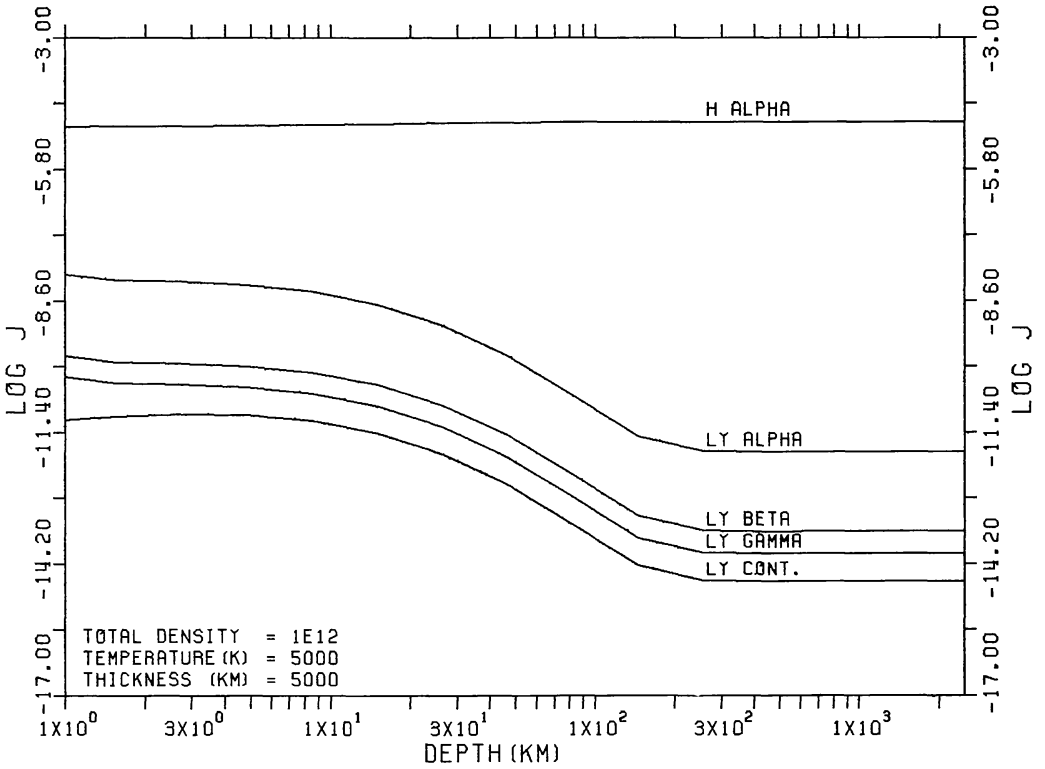

Fig. 1. Variation of radiation fields for hydrogen lines and continuum within the slab of a model prominence ($N = 10^{12}\ \mathrm{cm}^{-3}$, $T = 5000$ K, $D = 5000$ km). Abscissa represents the depth of a slab from the surface to the center (2500 km) and ordinate, mean intensities denoted by J.

© Kluwer Academic Publishers • Provided by the NASA Astrophysics Data System

1987SoPh..114...47K

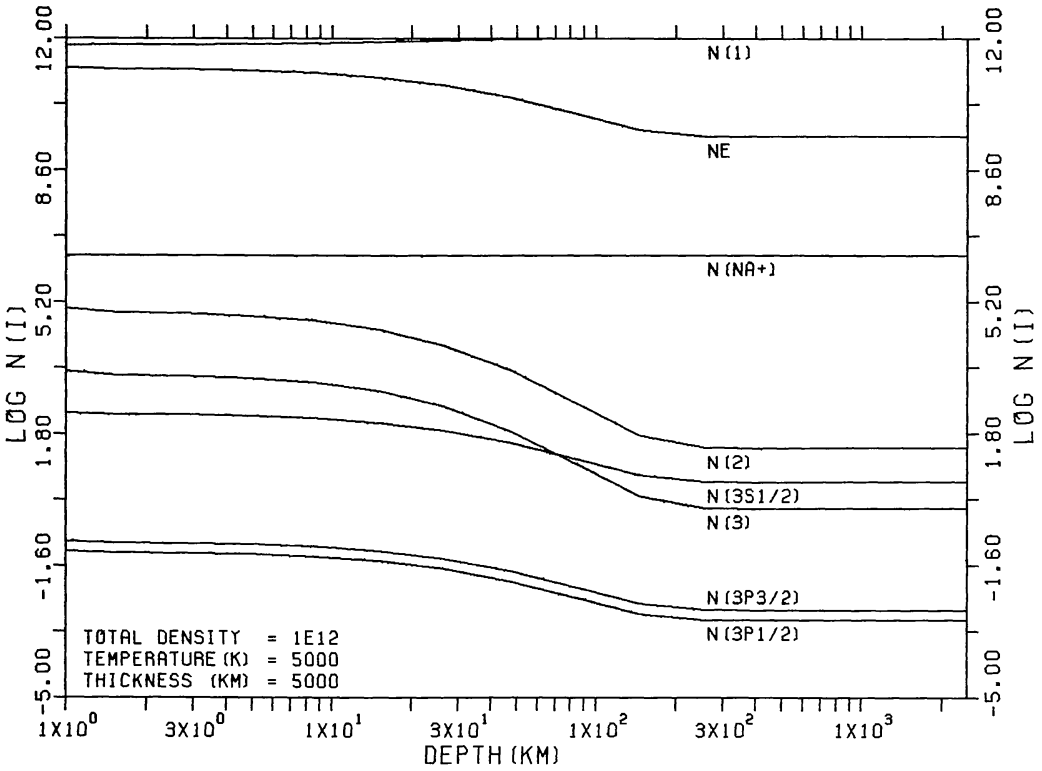

Fig. 2. Distribution of populations in the first three energy levels and continuum for the H and Na atoms, including the electron number. Model parameters in use are the same as in Figure 1.

dencies of radiation fields for Lyman lines and continuum including Hα line are shown in Figure 1, which indicates that all incident radiations penetrate into a substantial depth in the slab. Figure 2 shows the populations of hydrogen and sodium atoms in the first three energy levels and continuum. The variation pattern for the first three energy levels of sodium atom is the same as that for the free electron populations, implying that collisional recombinations of the ionized sodium with electrons are very dominant. As seen in the above figures, the most striking features are the very steep gradients in radiation fields and populations which occur close to the surface. These steep gradients arise from the considerable attenuation of the Ly continuum radiation to ionize hydrogen gas. We notice that sodium atoms are entirely ionized even at a temperature as low as 5000 K by EUV radiations, while almost all hydrogen atoms remain in the ground state, reflecting the large difference in ionization potentials between both atoms.

Keeping density and thickness of the model unchanged, we made the same analysis for a temperature of 8000 K. As shown in Figure 3 and 4, radiation fields and level populations change slowly with an inverse gradient compared to the previous low temperature model. As mentioned by Heasley and Milkey (1983), this can be understood by the fact that the radiation temperature ($\sim$6500 K) of Ly continuum incident on the surface runs close to the internal temperature at the central part of the model where its optical depth becomes large. Variations of source functions for Hα and D2 lines are plotted in Figure 5 with their contribution functions which are defined by the integrand

© Kluwer Academic Publishers • Provided by the NASA Astrophysics Data System

1987SoPh..114...47K

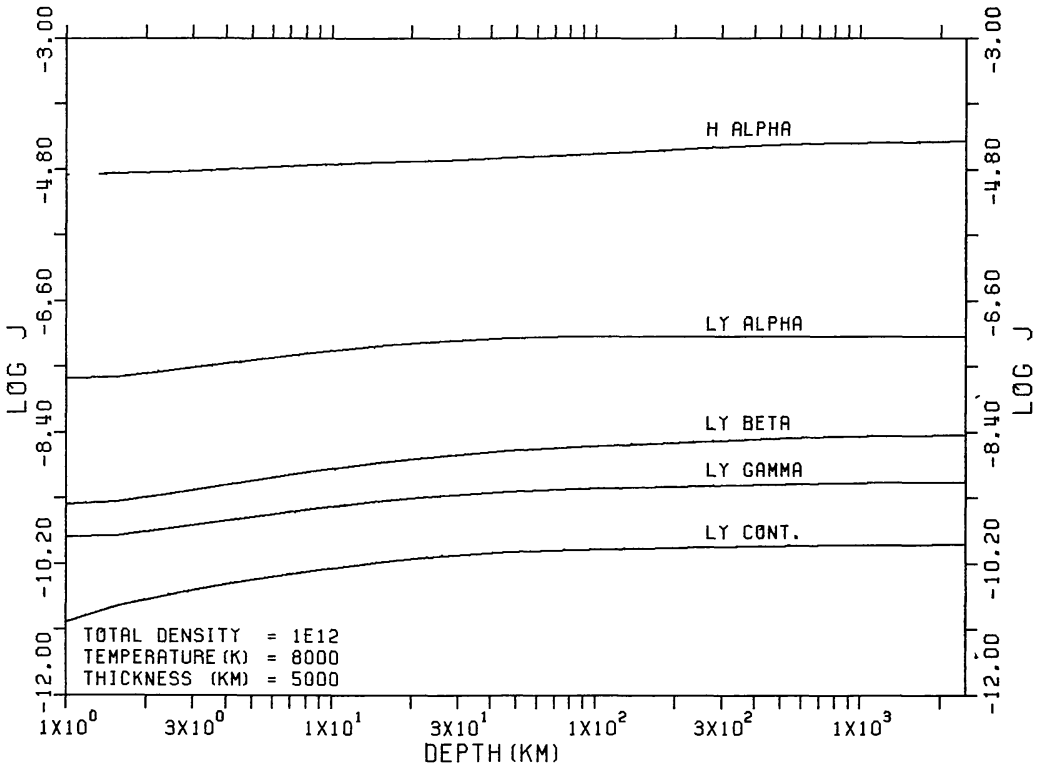

Fig. 3. Same as Figure 1 for the model prominence with the parameters of $N = 10^{12}$ cm^{-3}, $T = 8000$ K, and $D = 5000$ km.

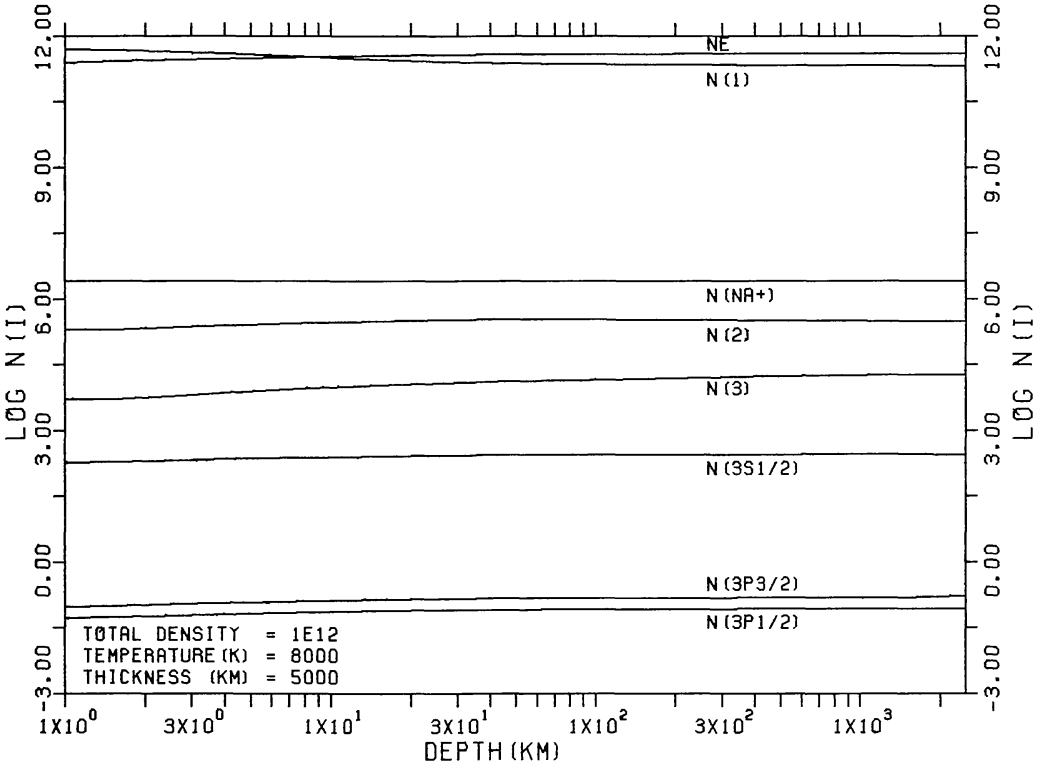

Fig. 4. Same as Figure 2 for the model prominence with the parameters of $N = 10^{12}$ cm^{-3}, $T = 8000$ K, and $D = 5000$ km.

© Kluwer Academic Publishers • Provided by the NASA Astrophysics Data System

1987SoPh..114...47K

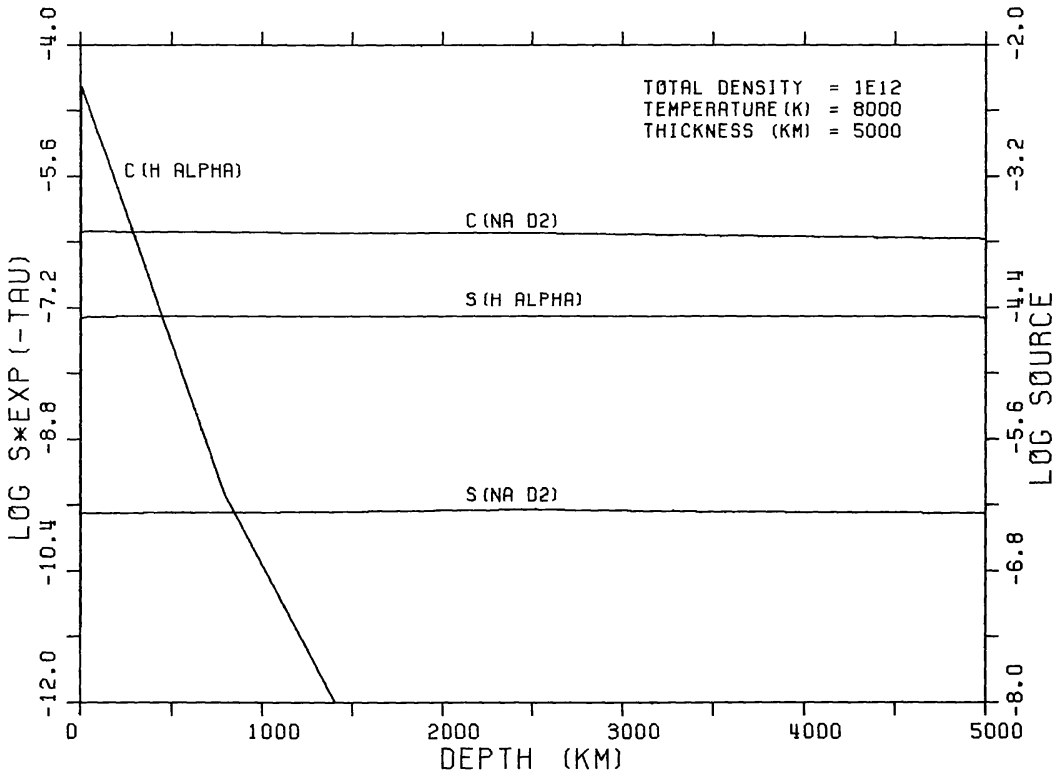

Fig. 5. Contribution and source functions for Hα and Na I D2 lines seen at the surface (0 km). Left-hand ordinate represents the contribution C defined by the integrand of Equation (5) and right-hand ordinate, the source S.

of Equation (5), $S(\tau)e^{-\tau}$. As shown in the figure, there are no changes in the source functions of Hα and Na I D2 lines. The contribution function for Hα line is large around the surface of the model, while that for the optically thin D2 line is practically constant throughout the interior. Such a different behavior of the contribution functions for both lines is due to the large difference in optical thicknesses of the lines.

The influence of geometry upon the line emission has been examined by considering the fine structure of prominences. That is, we divide the prominence model represented by one slab into a number of identical pieces with a given size and apply to each piece the same boundary conditions as assumed initially in the model calculations of Tables I and II. The radiative interaction between filaments is not taken into account in our work. Table III shows the results obtained under the assumption that n filaments with the same thickness are lined up in a column along the line-of-sight. D and n denote the geometrical thickness of individual filament in kilometers and the number of filaments standing in the line of sight direction, respectively. As seen in the table, there is no effect of the fine structure upon the ionization rate of hydrogen and the Na I D2 line intensity for the model with a temperature of 7000 K, because of the constant distribution of populations within the whole interior. However, for the model with a large change in the ionization rate from the surface to the center, we can expect an enhanced D2 intensity by considering the filamentary structure. For instance, the D2 intensity emitted

© Kluwer Academic Publishers • Provided by the NASA Astrophysics Data System

1987SoPh..114...47K

TABLE III

Effect of geometrical thickness on Na I D2 line

D (km)	n	T = 5000 K $\langle N_e \rangle$	N = 1E12 E(D2)	T = 7000 K $\langle N_e \rangle$	N = 1E12 E(D2)
5000	1	7.35E9	1.009E2	2.07E11	2.118E3
2500	2	7.98E9	1.096E2	2.07E11	2.117E3
1250	4	1.03E10	1.415E2	2.06E11	2.114E3
625	8	1.50E10	2.060E2	2.06E11	2.108E3
313	16	2.45E10	3.363E2	2.05E11	2.099E3
156	32	3.01E10	4.130E2	2.03E11	2.083E3

E(D2) is a total intensity of Na I D2 line emitted from n filaments with a thickness D standing in the line-of-sight direction.

$\langle N_e \rangle$ colums shows the change in the line-of-sight average of free electrons with the geometrical thickness of model filaments.

from a group of filaments (T = 5000 K, D = 156 km, and n = 32) is about 4 times higher than that from one slab model of D = 5000 km, because the number of free electrons from hydrogen atoms in a filament is highly increased by the geometrically thin structure.

We can make the Ly continuum radiation penetrate the filament more freely, by reducing its density. Figure 6 shows the distribution of radiation fields for a filament with

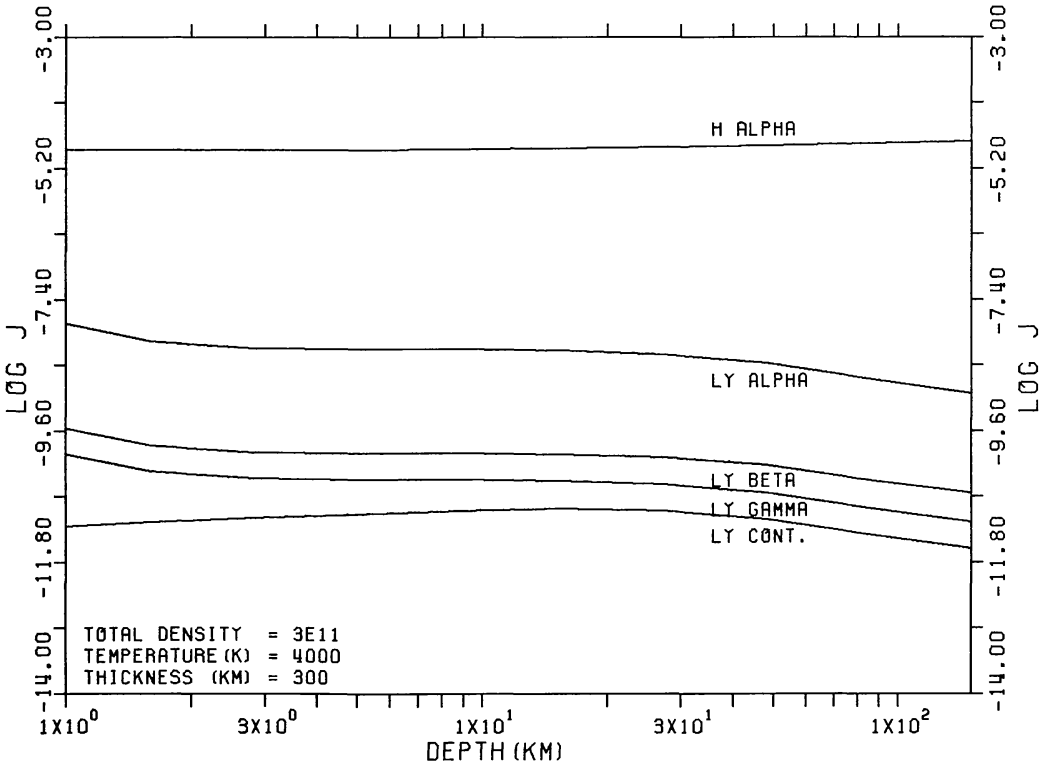

Fig. 6. Same as Figure 1 for the model prominence with the parameters of $N = 3 \times 10^{11}$ cm^{-3}, T = 4000 K, and D = 300 km.

© Kluwer Academic Publishers • Provided by the NASA Astrophysics Data System

1987SoPh..114...47K

a thickness of 300 km, a temperature of 4000 K and a density of 3×10^{11} cm^{-3} lower than in previous models. It is remarkable that the incident radiations pass through the whole interior without a large attenuation, for this model with a temperature as low as 4000 K. Although we can raise the ionization rate by reducing its density, strong Na I D line intensities are difficult to obtain. This is caused by the fact that the number of sodium atoms is reduced in proportion to the decrease of the total density.

In addition to the above mentioned facts, we find that the source function for Hα line is approximately constant, regardless of the density and the temperature. This property of constant source function for Hα is consistent with the result of Fontenla and Rovira (1985), and can be used very conveniently for the empirical analysis of the observed spectral line. For Na I D2 line, its optical thickness is so thin that the effect of radiative transfer may be negligible, except for the model case of extremely high density.

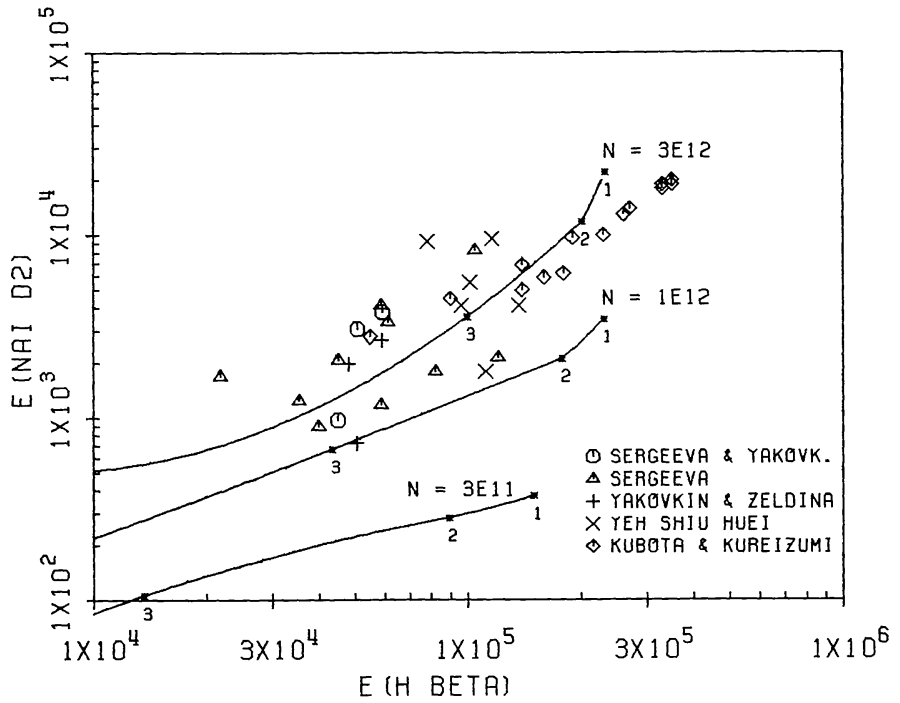

Fig. 7. Plot of observed Na I D2 integrated intensity against that for Hβ line. Full lines are the theoretical sequences calculated by models with a constant density of 3×10^{11}, 10^{12}, and 3×10^{12} cm^{-3}, and variable temperatures. Symbol * marked on the curved lines by 1, 2, and 3 represents the temperature of 8000, 7000, and 6000 K, respectively.

We have compared the results of our calculation with the observations. A plot of Na I D2 integrated intensity against that for Hβ line is shown in Figure 7. Symbols of ⏲, △, +, ×, and ◇ in the figure represent the spectral data observed by Sergeeva and Yakovkin (1964), Sergeeva (1968), Yakovkin and Zeldina (1974), Yeh (1961), and Kubota and Kureizumi (1986). respectively. We detect the observed proportionality between the Na I D2 line strength and the intensity of Hβ, as already found in Table II. We have attempted to match the observations with some of our models. Full lines in

© Kluwer Academic Publishers • Provided by the NASA Astrophysics Data System

1987SoPh..114...47K

Figure 7 are the theoretical sequences calculated by models with a constant density of 3×10^{11}, 10^{12} and 3×10^{12} cm^{-3}, and variable temperatures. Calculations for models with a density higher than 10^{12} cm^{-3} are in good agreement with the observations. On the contrary, low density models cannot fit well the observations, unless their thicknesses are assumed to be unreasonably large.

The electron density obtained from our models with a temperature higher than 6000 K generally lies in the range 10^{10}–4×10^{11} cm^{-3}, except for the model with $N = 3 \times 10^{12}$ cm^{-3} and $T = 8000$ K. This is nearly consistent with the result of Chultem and Yakovkin (1974) and Hirayama (1985). Much lower electron densities of $N_e \approx 7 \times 10^9$ cm^{-3} have been derived by Sahal-Brechot (1984) from the Hanle effect, but our models with a low electron density do not reproduce well the emissions of Na I D lines. Our ionization degree varies in the wide range 0.9–2×10^{-5}. Landman's value for the rate (0.16) corresponds roughly to the model with $N = 10^{11}$ cm^{-3} and $T = 6000$ K or $N = 3 \times 10^{12}$ cm^{-3} and $T = 7000$ K. For models with density higher than 10^{12} cm^{-3} and temperature above 7000 K, the calculated optical depth of Hβ exceeds 1 and τ(Hα) becomes very large, compared with observed values (10–60, Hirayama, 1964; 7–32, Yakovkin and Zeldina, 1974). Our calculated values of the intensity ratio of D1 to D2 line (~ 0.62) agree very well with the observed ratios shown in the work of Nikaido and Kawaguchi (1983).

4. Discussion

In our model calculations, we have assumed 7 bound levels plus continuum for the sodium atom. The truncation effects of remaining upper levels were pointed out by Landman (1986). He showed that the neglect of the upper level group ($> 5P$) in Na atom leads to roughly a factor of 2 underestimate in the evaluation of lower level populations. We admit that our calculated results on the total intensities of Na I D lines may be underestimated by a factor of about 2.

We will discuss the role of some physical parameters related closely to the sodium lines formation. The strength of sodium lines should be proportional primarily to the total amounts of sodium atoms along the line-of-sight in the excited states of $3P_{1/2,\,3/2}$ levels. Consequently, the total number density and the thickness of the slab are the major factors to control the intensities of Na I D lines.

In the statistical equilibrium solution, atomic populations are determined by the temperature, radiation fields and electron density. For a fixed number of total particles and electrons, the strength of Na I D lines increases as the temperature decreases, due to the corresponding rise of the populations in $3P_{1/2,\,3/2}$, including $3S_{1/2}$ level. In view of this fact, it is natural that Nikaido and Kawaguchi (1983) derive an emitting region with a low temperature (~ 4000 K) for strong Na I D lines, on the ground that they constructed the prominence model with a fixed electron density ($N_e = 0.1N$). Actually, however, free electrons vanish, in proportion to the decrease of the temperature, as shown in Table II. At the same time, emission of sodium lines falls down, as the number of electrons decreases with temperature.

© Kluwer Academic Publishers • Provided by the NASA Astrophysics Data System

1987SoPh..114...47K

We would like to emphasize here the role of free electrons in the formation of sodium D lines. Electrons, which are mainly supplied from hydrogen atoms ionized by Lyc radiation, are again recombined with ionized sodium, throughout dominant collisional recombination processes. As pointed out by Landman (1983), the magnitude of electron density yields the large populations in $3P_{1/2,\,3/2}$ levels including the ground level, according to the relation of $N(3P_j) \sim N_e N(\mathrm{Na}^+)$ depending slightly on the temperature. Thus if free electrons (or ionized sodium) are numerous, we can expect strong emissions in Na I D lines. Then, the number of electrons should be determined by the simultaneous equations of (1), (2), (3), and (4) in our work. Actual electron density calculated in this way has a strong dependence on the model parameters such as temperature and density, as shown in Table I. It is apparent that the ionization degree adopted in previous work (Nikaido and Kawaguchi, 1983) as a parametric independent value, should deviate largely from the real one for models of temperature below 7000 K.

This can be proved more evidently by the inspection of the variations of the ionization rate with temperature. Figure 8 shows the behavior of the ionization rate obtained by the non-LTE calculation of hydrogen. The rate is almost constant with a value of about 0.3 for the model with 7000 K, but at 4000 K the rate is so small that the total number of electrons supplied from hydrogen, even including the contribution from sodium are no more than 10^{-5} times of the total number of hydrogen atoms. Actually, great care must be paid when one estimates initially the electron density as a fixed value in non-LTE calculation of heavy elements.

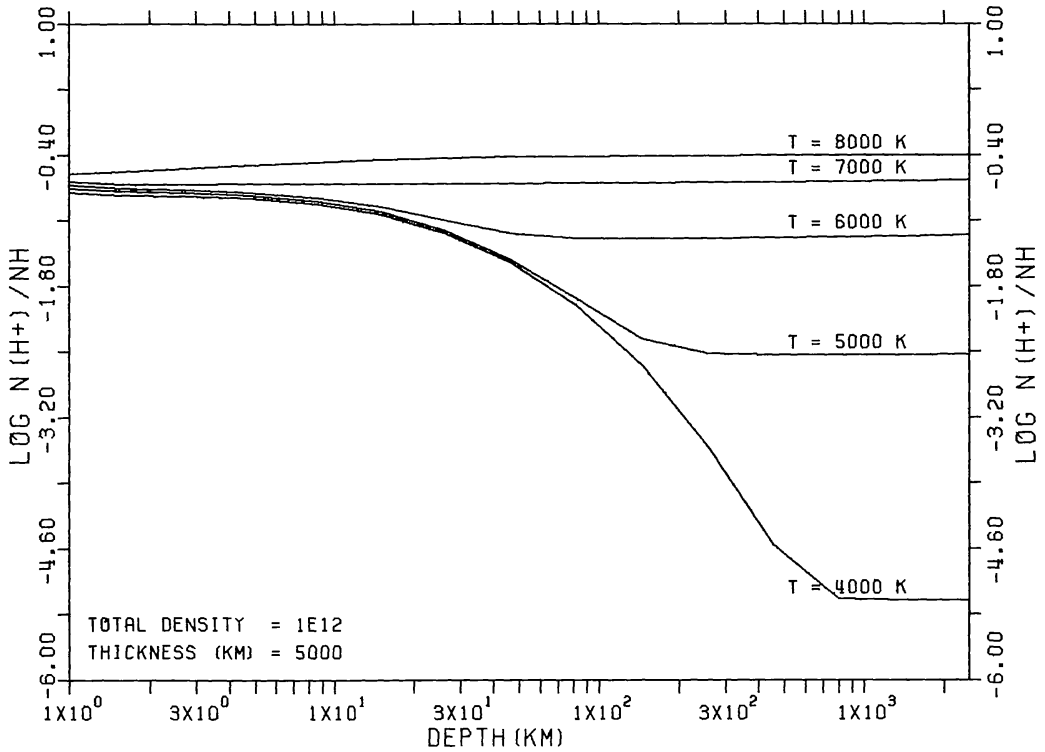

Fig. 8. Ionization ratio, $N(\mathrm{H}^+)/N(\mathrm{H\,I})$ of a model prominence ($N = 10^{12}$ cm^{-3}, $D = 5000$ km) for the various temperature values. $N(\mathrm{H}^+)$ and $N(\mathrm{H\,I})$ denote the number of ionized hydrogen (protons) and neutral hydrogen, respectively.

© Kluwer Academic Publishers • Provided by the NASA Astrophysics Data System

1987SoPh..114...47K

Provided that free electrons are abundant, it is expected that Na I D lines could be formed sufficiently, even in prominences with a temperature below 5000 K. We have attempted to increase the electron density by reducing the thickness of the slab. The expected increase of the ionization degree was obtained for a cool and dense model with a large change in radiation fields and populations from surface to center. Aside from changing the thickness, the decrease of total density also leads to the fair rise of the rate, due to the easier penetration of Lyc radiation. But the variation in strength of Na I D lines is insignificant, since total amounts of sodium atoms are depleted by lowering the total number density.

The strength of the EUV continuum radiation has a great influence on the ionization equilibrium of atoms. In our work, we used the continuum radiation field observed in quiet Sun. Solar EUV($\lambda < 912$ Å) and UV($\lambda < 2414$ Å) observational data show that the change of their continua from quiet regions to coronal holes is very small. However, we find that the Ly continuum intensity above active regions comes up to about 8 times of that above quiet ones, as shown in Vernazza and Reeves (1978), while the UV continuum ($\lambda < 2414$ Å) varies slightly throughout the two different regions. According to the calculation with the changed Ly continuum data, the number of free electrons from hydrogen is increased by a factor under 2 at the surface. For the most part of the interior, there is no change in the number of free electrons, since the variation of Ly continuum occurs only around the surface. Consequently, even if the continuum radiation data from an active region are used, the change in the line-of-sight average of free electron number $\langle N_e \rangle$ and the emission strength of Na I D lines is insignificant, compared to the quiet region.

Emergent intensities of Lyman lines wholly originate from the narrow sheath of prominences, due to the extremely large optical depths of those lines. In fact, our uniform models with a temperature lower than 8000 K cannot produce the central reversal of Lα and Lβ lines confirmed by satellite observations (Vial, 1982a), since the temperature in the vicinity of the surface is uniformly fixed to that of the cool core. If a realistic model structure with a steep temperature rise near the surface is considered, one can reproduce well the centrally reversed profile. Even for uniform models, reversed profiles can be obtained, if temperatures higher than 8000 K are assumed. Anyway, we would like to stress that our main concern is not a hot sheath where the Ly lines are formed but a cool core of the prominence to examine the emission of sodium lines.

In any case, numbers of prominence models with strong emission of Na I D lines are possible by the suitable combination of physical parameters. Among the numerous models supposed, we try to determine reasonable physical conditions for the Na I D lines emitting region, by using the observational constraints of Hα and Na I D lines in quiescent prominences. In fact, far more models must be simulated to examine the physical conditions which can reproduce well the observed quantities. Even though a sufficient number of examples has not been presented in our work, we can make the contour map which represents the iso-intensity of sodium D2 line and the iso-optical thickness of Hα line, by an interpolation based on our results of model calculations.

Figure 9 shows the diagnostic diagram on the physical conditions of the emitting

© Kluwer Academic Publishers • Provided by the NASA Astrophysics Data System

1987SoPh..114...47K

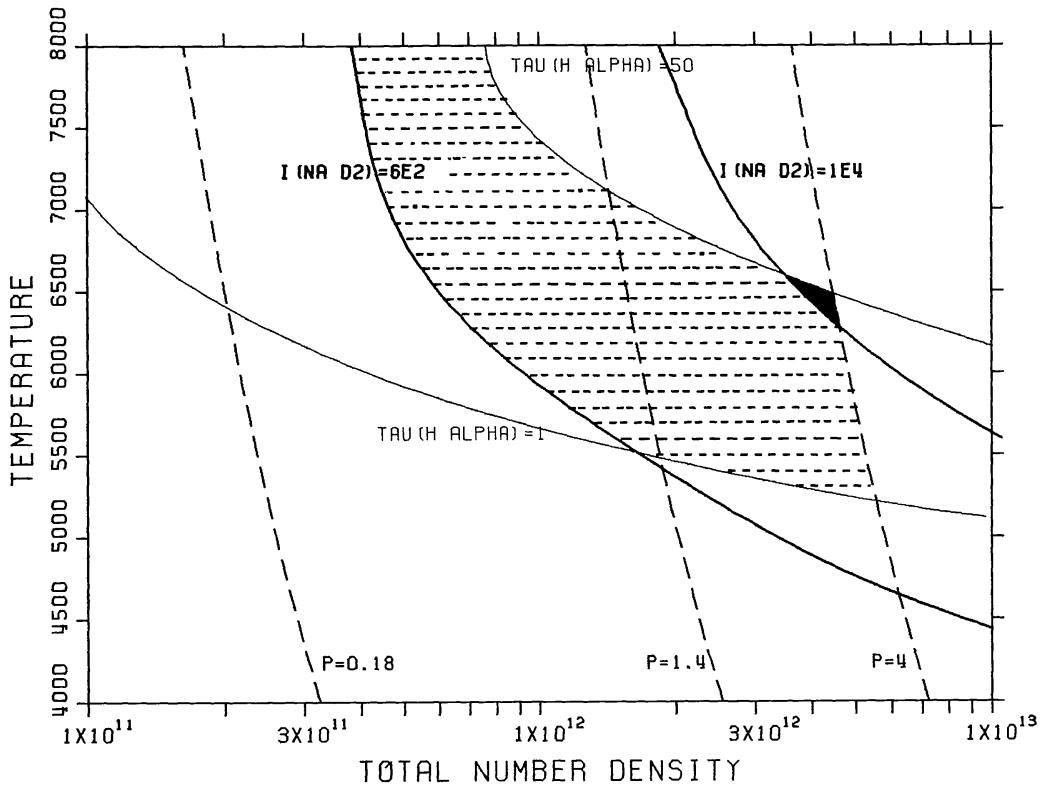

Fig. 9. Diagnostic diagram for the spectral emission of Hα and Na I D2 lines in prominences. Thin, thick and dashed lines represent the iso-contours of optical depths for Hα, intensities for Na I D2 line and gas pressures, respectively.

region in model prominences with the fixed thickness of 5000 km. Thin lines in the figure represent the contours for iso-optical depth of Hα with value of 1 and 50. The band formed by those lines stand for the physical conditions of Hα line emitting region in prominences, which belong to the range of the observational constraints for the line. Contours of iso-intensity of Na I D2 line with 6×10^2, and 10^4 ergs cm^{-2} s^{-1} $ster^{-1}$ are drawn in the figure with thick lines. Since the intensity of Na I D2 line observed in quiescent prominences lies in the range $6 \times 10^2 - 10^4$ ergs cm^{-2} s^{-1} $ster^{-1}$, the emitting region of sodium lines in quiescent prominences should be located in the zone enclosed by the contour lines. We also carry out the check of the gas pressure of prominence models. As drawn with dashed lines in the figure, the isobaric line corresponding to the coronal pressure value of 0.18 dyn cm^{-2} lies outside the Na I D2 line emitting region. It is certain that Na I D lines with an appreciable strength should be emitted in the high pressure region on the diagnostic diagram. Referring to the results of Landman (1983, 1984), we restrict the upper boundary of the pressure for our models to 4 dyn cm^{-2}. As shown in Figure 9, physical conditions of Hα and Na I D lines emitting regions, which satisfy both optical and physical constraints in quiescent prominences, are situated within the range represented by the shaded area. Small filled area represents the physical conditions where quiescent prominences can emit the strong

© Kluwer Academic Publishers • Provided by the NASA Astrophysics Data System

1987SoPh..114...47K

NaI D lines with an intensity over 10^4 ergs cm^{-2} s^{-1} $ster^{-1}$. In fact, such a strong emission of D lines may be infrequent in quiescent prominences.

From the above diagnostic diagram, we can estimate that sodium D lines are difficult to be formed in the cool core of prominence with a temperature below 5000 K. In order that the cool part of the prominence with a pressure below 4 dyn cm^{-2} emit the sodium D lines with an intensity between 6×10^2 and 10^4 ergs cm^{-2} s^{-1} $ster^{-1}$, along with a Hα optical depth between 1 and 50, a density higher than 4×10^{11} cm^{-3} and a temperature over 5000 K are necessary at least. Our conclusions on the emitting region of sodium lines are supported implicitly by Landman's results (1983, 1984) for the principal plasma parameters derived from the empirical analysis of optically thin lines including NaI D lines.

Acknowledgements

The author would like to express his gratitude to Prof. Kawaguchi and a referee for their helpful discussions and criticisms, which led to a number of improvements in this paper. He is also indebted to the members of the Kwasan and Hida Observatories for their supports on this work, during his stay in Japan.

References

Auer, L. H. and Mihalas, D.: 1969, *Astrophys. J.* **158**, 641.
Chultem, T. and Yakovkin, N. A.: 1974, *Solar Phys.* **34**, 133.
Dunn: 1960, Ph. D. Thesis, Harvard University.
Engvold, O.: 1978, *Solar Phys.* **64**, 177.
Fontenla, J. M. and Rovira, M.: 1983, *Solar Phys.* **85**, 141.
Fontenla, J. M. and Rovira, M.: 1985, *Solar Phys.* **96**, 53.
Heasley, J. N. and Mihalas, D.: 1976, *Astrophys. J.* **205**, 273.
Heasley, J. N., Mihalas, D., and Poland, A. I.: 1974, *Astrophys. J.* **192**, 181.
Heasley, J. N. and Milkey, R. W.: 1976, *Astrophys. J.* **210**, 827.
Heasley, J. N. and Milkey, R. W.: 1978, *Astrophys. J.* **221**, 677.
Heasley, J. N. and Milkey, R. W.: 1983, *Astrophys. J.* **268**, 398.
Hirayama, T.: 1964, *Publ. Astron. Soc. Japan* **15**, 122.
Hirayama, T.: 1985, *Solar Phys.* **100**, 415.
Kawaguchi, I.: 1964, *Publ. Astron. Soc. Japan* **16**, 86.
Kubota, J. and Kureizumi, T.: 1986, *Contr. Kwasan and Hida Obs.*, No. 274.
Landman, D. A.: 1981, *Astrophys. J.* **251**, 768.
Landman, D. A.: 1983, *Astrophys. J.* **270**, 265.
Landman, D. A.: 1984, *Astrophys. J.* **279**, 483.
Landman, D. A.: 1985, *Astrophys. J.* **290**, 369.
Landman, D. A.: 1986. *Astrophys. J.* **305**, 546.
Lambert, D. L. and Luck, R. E.: 1978, *Monthly Notices Roy. Astron. Soc.* **183**, 79.
Mihalas, D.: 1967, *Astrophys. J.* **149**, 169.
Mihalas, D.: 1978, *Stellar Atmospheres*, W. H. Freeman and Co, San Francisco.
Mihalas, D., Auer, L. H., and Mihalas, B. R.: 1978, *Astrophys. J.* **220**, 1001.
Milkey, R. W., Heasley, R. N., Schmahl, E. J., and Engvold, O.: 1979, *IAU Colloq.* **44**, 53.
Nikaido, Y. and Kawaguchi, I.: 1983, *Solar Phys.* **84**, 49.
Pierce, A. K. and Slaughter, C.: 1982, *Astrophys. J. Suppl. Ser.* **48**, 73.
Poland, A. I., Skumanich, A., Athay, R. G., and Tandberg-Hanssen, E.: 1971, *Solar Phys.* **18**, 391.

© Kluwer Academic Publishers • Provided by the NASA Astrophysics Data System

1987SoPh..114...47K

Sahal-Brechot, S.: 1984, *Ann. Phys. France* **9**, 705.
Sampson, D. H. and Golden, L. B.: 1970, *Astrophys. J.* **161**, 321.
Sergeeva, A. N.: 1968, *Vestnik Kievskovo Universiteta, Ser. Astron.*, No. 10, 3–14.
Sergeeva, A. N. and Yakovkin, N. A.: 1970, *Vestnik Kievskovo Universiteta, Ser. Astron.*, No. 12, 3–10.
Vernazza, J. E. and Reeves, E. M.: 1978, *Astrophys. J. Suppl. Ser.* **37**, 485.
Vial, J. C.: 1982a, *Astrophys. J.* **253**, 330.
Vial, J. C.: 1982b, *Astrophys. J.* **254**, 780.
Wiese, W. L., Smith, M. W., and Glennon, B. W.: 1966, *Atomic Transition Probabilities*, U.S. Government Printing Office, Washington.
Yakovkin, N. A. and Zeldina, M. Y.: 1974, *Soviet Astron. AJ* **7**, 643.
Yeh, S. H.: 1961, *Izv. Krymsk. Astrofiz. Obs.* **25**, 180.

© Kluwer Academic Publishers • Provided by the NASA Astrophysics Data System